# Chapter 2

## Effect of Head Group Polarity on Aggregation Properties of Dimeric Surfactants

# Contents

## 2.1 Introduction

Classical surfactant molecules are generally composed of two distinct parts: polar head and alkyl chain, incompatible with one another. They are known for their tendency to self-associate and give rise to well developed superamolecular assemblies, called micelles. The micelles formed are of various types, shapes and sizes, such as globular, cylindrical and spherical. The characteristics of these aggregates are governed by the molecular structure of the surfactant molecules as well as by physical parameters such as concentration, temperature and ionic strength [1-5].

Hence attempts to design newer molecular structures with greater surface activity led to the preparation of new generation surfactants such as geminis. A conventional surfactant has a single hydrophobic tail connected to an ionic or polar head group, whereas a gemini has in sequence a long hydrocarbon chain, an ionic group, a spacer, a second ionic group and another hydrocarbon tail. A schematic representation of a gemini is shown below.

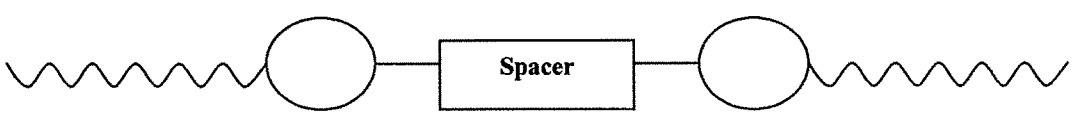


Geminis are considerably more surface active than conventional monomeric surfactants. All geminis possess at least two hydrophobic chains and two ionic or polar head groups and a spacer [6]. Spacer can be flexible, rigid, polar or non-polar in nature. Flexible spacer may be of short or long chain of methylene groups. Rigid spacers can be of stilbene type. Polar spacers may contain polyethers and non-polar spacers may be of acetylenic type. The ionic group can be positively charged (ammonium) or negatively charged (phosphate, sulfate, carboxylate) whereas the polar nonionics may be polyether or sugar.

The majority of geminis have symmetrical structures with two identical polar groups and two identical chains. Some unsymmetrical geminis and geminis with three or more polar groups or tails have recently been reported [7-11]. The bis-quaternary surfactants with general molecular formula $C_nH_{2n+1}N^+(CH_3)_2$—$(CH_2)_s$—$N^+(CH_3)_2C_nH_{2n+1}$, $2Br^-$ are referred as m-s-m DMA (DMA = Dimethyl ammonium bromide) surfactants[12]. These surfactants, because of their unique solution properties such as very low CMC, high detergency, high solubilization and high surface wetting capacity, possess wide range of applications in diverse industries such as mining, petroleum, chemical, pharmaceutical, in biochemical research [13] and as catalysts in several chemical reactions[14]. They are also used as preservatives [15], anticorrosive [16,17] and antimicrobial agents[18,19]. Currently these gemini surfactants have attracted more attention as potential gene delivery agents [20,21], as erythrocyte protectors against hypotonic heamolysis [22] and as templates in synthesis of new mesoporus zeolites MCM-41 and MCM-48 [23-25].

Increased interest in these surfactants can be attributed to the ease with which desired physicochemical properties can be obtained just by varying the solution composition [26,27]. The various physicochemical properties of surfactants were reported to be much sensitive to molecular architecture and environmental conditions such as temperature, pressure and additives [28-35].

- In 1996 Rosen and Song[36,37] reported on the micellization and premicellization behavior of a series of biscationic surfactants with rigid hydrophobic and flexible hydrophilic spacers. A higher aggregation tendency was reported for a gemini surfactant with flexible hydrophilic spacer than gemini with rigid hydrophobic spacer
- Zana and Talmon [38-39] have also reported, influence of change in spacer length, nature (hydrophilic / hydrophobic) and its flexibility on performance properties of gemini surfactants.

- Recently Wettig et al [40-42] studied the effect of hydrophilic spacer on aggregation pattern and physicochemical properties of bis (dodecyl dimethyl ammonium bromide) surfactant.
- Zana [43], and Menger and Keiper [44] have reported that the aggregation and thermodynamic properties of series of dimeric surfactants with alkyl tail of fixed carbon length depend on the conformation of spacer chain.
- Halder et al[45] reported the aggregation properties of novel cationic surfactants with multiple pyridinium head groups, through SANS and observed that aggregation number (*N*) dramatically decreased with increase in the number of head groups.

However, the effect of variation in the head group polarity (which can offer interesting physicochemical properties) on the properties of cationic gemini surfactants, has not been systematically studied so far. Hence in this chapter results obtained in the study of the effect of variation in head group polarity on physicochemical properties of bis(dodecyldimethylammonium bromide) surfactant with four methylene spacer chain are presented.

## 2.2 Experimental

### 2.2.1 Synthesis and Characterization of Cationic Surfactants

**Materials**

Dodecyl bromide, dihydroxyethylmethyl amine, hydroxyethyldimethyl amine, dodecyltrimethylammonium bromide (DTAB), dimethyl amine, hydroxyethylmethyl amine, dihydroxyethyl amine and 1, 4-dibromo butane were purchased from Lancaster, Morecambe, England. Solutions for SANS studies were prepared in $D_2O$ (at least 99 atom % D) obtained from Heavy Water Division, Bhabha Atomic Research Centre, Mumbai, India. Double-distilled and deionized water was used for all physicochemical studies.

**Synthesis**

The dimeric surfactants were synthesized by refluxing 2.2 moles of dodecyl dimethyl amine / dodecyl hydroxyethylmethyl amine / dodecyl dihydroxyethyl amine in dry acetone with 1.0 mole of 1,4-dibromo butane for 70 h., at 60 °C.

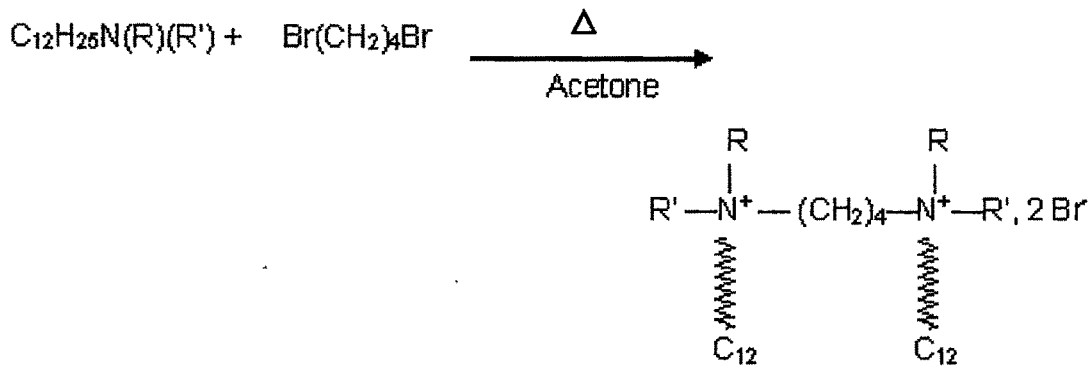


Abbreviations used in surfactant nomenclature are

| | |
|---|---|
| $R = R' = CH_3$ | : 12-4-12 DMA |
| $R = CH_3$ and $R' = C_2H_4OH$ | : 12-4-12 MEA |
| $R = R' = C_2H_4OH$ | : 12-4-12 DEA |

The solvent from reaction mixture was removed under vacuum and the crude white solid thus obtained was purified by washing with hexane/ethyl acetate mixture and recrystallized from acetone/methanol mixture for at least three times to obtain pure compound. The overall yield of the surfactant was observed to be 75-80 %.

**Structures, abbreviations and nomenclature of bis-cationic surfactants under study**

(a) *Butanediyl-1,4-N,N'-bis(N,n-dodecyl N-dimethylammonium bromide)* represented as 12-4-12 DMA (DMA = dimethyl amine)

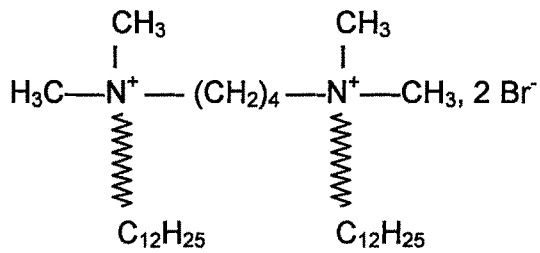


(b)*Butanediyl-1,4-N,N'-bis(N,n-dodecyl N-hydroxyethyl N-methylammonium bromide)* represented as 12-4-12 MEA ( MEA = monoethanol amine)

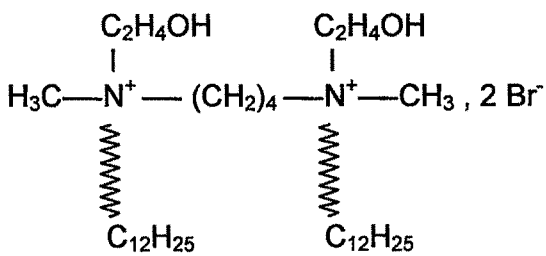


(c) *Butanediyl-1,4-N,N'-bis(N,n-dodecyl N-dihydroxyethylammonium bromide)* represented as 12-4-12 DEA (DEA = diethanol amine)

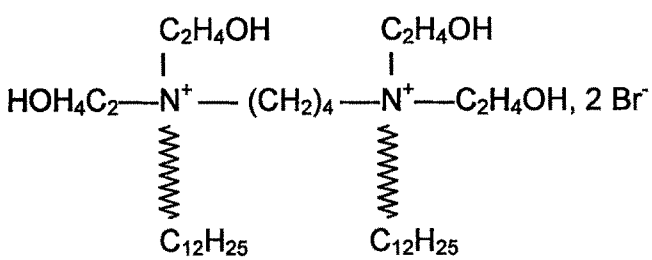


(d) *Dodecyl hydroxyethyl dimethyl ammonium bromide*

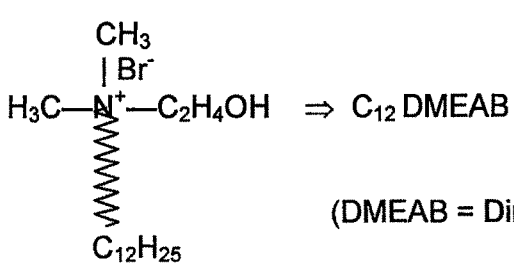


⇒ $C_{12}$ DMEAB

(DMEAB = Dimethyl ethanol ammonium bromide)

(e) ***Dodecyl dihydroxyethyl methyl ammonium bromide***

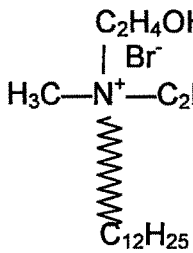

$\Rightarrow C_{12}$ DEMAB

(DEMAB = Diethanol methyl ammonium bromide)

(f) ***Dodecyl trimethyl ammonium bromide***

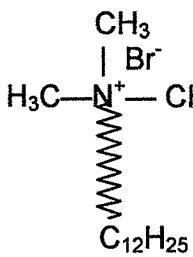

$\Rightarrow C_{12}$TMAB (DTAB) commercially available

(TMAB = Tri methyl ammonium bromide)

The purity and structure of the synthesized surfactant molecules were checked by TLC, FTIR (Perkin Elmer-RX1), $^1$H NMR (Bruker 300 $MH_Z$) and elemental analysis (Perkin Elmer Series II). The details of the results are given below.

**(a)** *Butanediyl-1,4,-N,N'-bis(N,n-dodecyl N-dimethylammonium bromide)* represented as 12-4-12 DMA, **:** The infrared spectrum of surfactant exhibited absorption bands at 2916 $cm^{-1}$ corresponding to –CH stretching, at 1108 $cm^{-1}$ corresponding to –CN stretching and at 720 $cm^{-1}$ due to –CH rocking from long alkyl chain $-(CH_2)_n$.

$^1$H NMR spectrum of surfactant showed signals at δ 0.85 ppm ( t, 6H, 2 x $CH_3$ alkyl chain ), 1.24-1.74 ppm (br m, 40H, 20 $CH_2$ alkyl chain), 2.1 ppm (br, m, 4H, $2CH_2$ spacer chain), 3.29 ppm (s,12H, $4N^+CH_3$), 3.44 ppm (t, 4H, 2 x $N^+$-$CH_2$ alkyl chain), 3.86 ppm (t, 4H, 2 x $N^+$-$CH_2$, spacer chain ).

C, H, N percentage, calculated for $C_{32}H_{70}N_2Br_2$ was C: 59.80, H: 10.99, N: 4.36 and experimentally found was C: 59.98, H: 11.39, N: 4.47.

Melting point of the surfactant was observed to be 200 $\pm$ 2°C.

**(b)** *Butanediyl-1,4,-N,N'-bis(N,n-dodecyl N-hydroxyethyl N-methylammonium bromide)* represented as 12-4-12 MEA : The infrared spectrum of surfactant showed broad absorption bands at 3401-3656 $cm^{-1}$ due to –OH stretching, at 2917 $cm^{-1}$ due to –CH stretching, at 1105 $cm^{-1}$ corresponding to –CN stretching, at 1085 $cm^{-1}$ due to –CO stretching and at 721 $cm^{-1}$ due to –CH rocking from long alkyl chain $-(CH_2)_n$.

$^1H$ NMR spectrum of surfactant showed signals at δ 0.84 ppm (t, 6H, 2 x $CH_3$ alkyl chain), 1.25 - 1.40 ppm (br, m, 36H, 18 $CH_2$ alkyl chain), 1.75 ppm (br m, 4H, $2CH_2$ alkyl chain), 2.1 ppm (m, 4H, $2CH_2$ spacer chain), 3.25 ppm (s, 6H, 2 $N^+CH_3$), 3.62 ppm (t, 12H, 2 x $N^+(CH_2)_3$), 3.82 ppm (t, 4H, $2CH_2$-OH ), 4.18 ppm ( s, 2H, 2-OH ).

C, H, N, percentage calculated for $C_{34}H_{74}N_2O_2Br_2$ was C: 58.10, H: 10.61, N: 3.98 and experimentally found was C: 58.20, H: 10.75, N: 4.01.

Melting point of the surfactant was observed to be 196 $\pm$2 °C.

**(c)** *Butanediyl-1,4,-N,N'-bis(N,n-dodecyl N-dihydroxyethylammonium bromide)* represented as 12-4-12 DEA: The infrared spectrum of surfactant showed broad absorption bands at 3401-3665 $cm^{-1}$ due to –OH stretching, at 2917 $cm^{-1}$ due to –CH stretching, at 1103 $cm^{-1}$ corresponding to –CN stretching, at 1083 $cm^{-1}$ due to –CO stretching and at 721 $cm^{-1}$ due to –CH rocking from long alkyl chain $-(CH_2)_n$.

$^1H$ NMR spectrum of surfactant showed signals at δ 0.80 ppm (t, 6H, 2 x $CH_3$ alkyl chain), 1.17-1.24 ppm (br m,36H, 18 $CH_2$ alkyl chain), 1.63 ppm (br m, 4H, $2CH_2$ alkyl chain), 1.87 ppm (m, 4H, $2CH_2$ spacer chain), 3.04 ppm ( t, 16H, 2 x $N^+(CH_2)_4$), 3.88 ppm ( t, 8H, 4 $CH_2$-OH ), 5.17 ppm (s, 4H, 4-OH ).

C, H, N percentage calculated for $C_{36}H_{78}N_2O_4Br_2$ was C: 56.71, H: 10.24, N: 3.68 and experimentally found was C: 57.28, H: 10.58, N: 3.69.

Melting point of surfactant was observed to be 190 $\pm$ 2 °C.

**(d)** *N,n-dodecyl hydroxyethyl dimethyl ammonium bromide*
represented as $C_{12}$ **DMEAB**: The infrared spectrum of surfactant showed broad absorption bands at 3400-3633 $cm^{-1}$ due to –OH stretching, at 2911 $cm^{-1}$ due to –CH stretching, at 1100 $cm^{-1}$ corresponding to –CN stretching, at 1053 $cm^{-1}$ due to –CO stretching and at 721 $cm^{-1}$ due to –CH rocking from long alkyl chain $-(CH_2)_n$.

$^1H$ NMR spectrum of surfactant showed signals at δ 0.83 ppm (t, 3H, $CH_3$ alkyl chain), 1.19 ppm (br m,14H, $7CH_2$ alkyl chain), 1.69 ppm (br m, 6H, $3CH_2$ alkyl chain), 3.31 ppm (s, 6H, 2 x $N^+CH_3$), 3.46 ppm ( t, 2H, $N^+CH_2$ alkyl chain), 3.67 ppm ( t, 2H, $N^+CH_2$), 4.04 ppm (t, 2H, $CH_2$-OH), 4.42 ppm (s, H, OH ).

C, H, N calculated percentage for $C_{16}H_{36}NOBr$ was C: 56.79, H: 10.72, N: 4.14 and experimentally found was C: 56.85, H: 10.78, N: 4.20.

Melting point of surfactant was observed to be 165 ± 2 °C.

**(e)** *N,n-dodecyl dihydroxyethyl methyl ammonium bromide,* represented as $C_{12}$**DEMAB** : The infrared spectrum of surfactant showed broad absorption bands at 3401-3645 $cm^{-1}$ due to –OH stretching, at 2913 $cm^{-1}$ due to–CH stretching, at 1100 $cm^{-1}$ corresponding to –CN stretching, at 1065 $cm^{-1}$ due to –CO stretching and at 721 $cm^{-1}$ due to –CH rocking from long alkyl chain $-(CH_2)_n$.

$^1H$ NMR spectrum of surfactant showed signals at δ 0.83 ppm (t, 3H, $CH_3$ alkyl chain), 1.19 ppm (br m,14H, $7CH_2$ alkyl chain), 1.69 ppm (br m, 6H, $3CH_2$ alkyl chain), 3.31 ppm (s, 3H, $N^+CH_3$), 3.46 ppm ( t, 2H, $N^+CH_2$ alkyl chain), 3.67 ppm ( t, 4H, $N^+CH_2$), 4.04 ppm (t, 4H, $2CH_2$-OH), 4.42 ppm (s, 2H, 2OH ).

C, H, N percentage calculated for $C_{17}H_{38}NO_2Br$ was C: 55.43, H: 10.40, N: 3.80 and experimentally found was C: 55.94, H: 10.65, N: 4.00.

Melting point of surfactant was observed to be 170 ± 2 °C.

### 2.2.2 Kraft Temperature

Kraft temperature ($k_T$) of the bis-cationic (12-4-12 DMA) surfactant was measured as a function of increase in the number of $-C_2H_4OH$ groups at quaternary amine group. Clear aqueous one percent (w/v) solution of surfactant was stored at 2 - 4°C for at least 45 - 48 h, until precipitate of the hydrated surfactant crystals appeared. The temperature of the precipitated system was gradually raised using water bath of accuracy of $\pm$ 0.1°C. The conductance was recorded as a function of increase in temperature. The $k_T$ was taken as the temperature where the conductance versus temperature plot showed an abrupt change in slope. Representative plot for determination of Kraft temperature for 12-4-12 MEA gemini surfactant is given in Figure 2.1. The experiments were repeated at least three times.

### 2.2.3 Conductivity

Critical micelle concentration of the surfactant was determined through conductance measurement using Digital Conductivity Meter-664 (Equiptronic, Mumbai, India) with conductivity cell of cell constant 1.01$cm^{-1}$ at 30 $\pm$0.1°C. The conductance of a series of solutions prepared by addition of an aliquot of a known concentration of surfactant solution to a given volume of the thermostated solvent was measured. Plots of specific conductance (k) against concentration (C) are given in Figure 2.2 (a, b. c) and 2.3 (a, b. c). The average degree of ionization ($\alpha_{ave}$) of a micelle was taken as the ratio of the values of dk/dC above and below the CMC.

### 2.2.4 Dye Adsorption

The absorption spectra were recorded with a Jasco V-530, Japan UV-visible spectrophotometer using a matched pair of glass cuvettes of 1 cm optical length placed in thermostated cell holder, at 30 $\pm$ 0.2°C. The concentration of bromo phenol blue dye (2 x $10^{-5}$ M) was kept constant. The absorbance was measured

at $\lambda_{max}$ of dye, 590 nm, in the presence of varying concentration of surfactant. Plots of the absorbance against surfactant concentration are given in Figure 2.3 (a, b, c).

### 2.2.5 Surface Tension

The reduction in surface tension ($\gamma$) with respect to surfactant concentration was measured by ring method using a du-Nouy tensiometer (S. C. Dey and Co., Kolkata, India) at 30±0.1°C. The temperature was maintained constant by circulating thermostated water through jacketed vessel containing the solution. Surface tension ($\gamma$) decreases quit rapidly with increasing surfactant concentration before reaching a near plateau region. The concentration of solution was varied by adding aliquots of concentrated stock solution to a known volume of solution in the jacketed vessel by means of a 5 µl Hamilton micro syringe. The ring was thoroughly cleaned between each measurement of surface tension. The measured surface tension values were plotted as a function of the concentration and the CMC was estimated from the break point in the resulting curve. The plots of surface tension ($\gamma$) against concentration (C) are given in Figure 2.2 (a, b, c).

### 2.2.6 Viscosity

The viscosity of aqueous surfactant solutions was measured by using Schott Gerate AVS-350 (Germany) Ubbelohde Internal Dilution Viscometer. During the measurements the viscometer was immersed in digital constant temperature water bath model CT-1650 Schott Gerate (Germany)maintained with an accuracy of ± 0.01°C and the flow time was recorded within accuracy of ± 0.02 s. Solutions were allowed to attain bath temperature by suspending viscometer, containing solution, for 30 min in water bath prior to the measurements.

### 2.2.7 Density

The densities of aqueous surfactant solutions were measured by using high precision Anton Paar Densitometer DMA-5000. The measured densities were accurate up to $\pm$ 0.000001 g $cm^{-3}$ and the temperature in the measuring cell was measured with an accuracy of $\pm$ 0.001 $^{0}C$ with built-in integrated Pt 100 measuring sensor.

### 2.2.8 Foamability

Foamability and foam stability of 12-4-12 DMA gemini surfactant as a function of head group polarity were studied as per method reported by Shah [46]. A graduated glass cylinder of 100 $cm^3$ volume was used for foam stability and foamability measurements. Twenty $cm^3$ 1 % (w/v) surfactant solution was poured into the calibrated cylinder. The solution was given 10 uniform jerks within 10 s. The volume of the foam generated was measured as foamability and the time required for the collapse of the foam to half its initial height was taken as a measure of foam stability. The experiments were repeated at least five times.

### 2.2.9 Small Angle Neutron Scattering

Small angle neutron scattering (SANS) measurements is a powerful technique for studying the shape, size and microenvironment of surfactant aggregates in aqueous solution [47,48]. SANS measurements of surfactant solutions were carried out as a function of head group polarity and spacer chain length, using a SANS Diffractometer at the Dhruva Reactor, Bhabha Atomic Research Center (BARC), Trombay, Mumbai, India [49]. All the surfactant solutions used for SANS studies were prepared in $D_2O$. The use of $D_2O$ instead of $H_2O$ provides very good contrast between surfactant aggregates and solvent in a SANS experiments. The sample to detector distance was 1.85 m for all the runs. This spectrometer contained BeO filtered beam and had a resolution ($\Delta Q/Q$) of about 15 % at Q = 0.05 $Å^{-1}$. The angular distribution of scattered neutron was recorded

using one-dimensional position sensitive detector (PSD). The range of wave vector transfer (Q) of this instrument was 0.018 – 0.30 $Å^{-1}$ and is given as $4\pi\sin\theta/\lambda$, where $\lambda$ is the wavelength of the incident neutron and $2\theta$ is the scattering angle. The detector allows a simultaneous recording of data over full Q range. The wave length of incident neutron ($\lambda$) was 5.2 Å. The solutions were held in a 0.5 cm path length UV grade quartz sample holder with tight fitting Teflon stopper sealed with para-film. The measured scattering intensities of neutron were corrected for background and empty cell scattering and sample transmission. Solvent intensity was subtracted from that of the sample. The intensities were normalized to absolute cross-section units and plots of coherent differential cross-section ($d\Sigma/d\Omega$) vs Q were obtained. The uncertainty in the measured scattering intensities was estimated to be < 10 %.

## 2.3 Results and Discussion

### 2.3.1 Kraft temperature

Kraft temperatures ($k_T$) of series of gemini surfactants 12-4-12 DMA/MEA/DEA and their monomeric counterparts $C_{12}$TMAB, $C_{12}$DMEAB, $C_{12}$DEMAB were measured through conductance measurements as described earlier. The Kraft temperature was determined from the plot of specific conductance vs temperature as shown in Figure 2.1. The conductance was observed to increase rapidly with increase in temperature due to dissolution of the hydrated crystals of surfactant until Kraft temperature reaches. Thereafter the conductance increases slowly due to only increase in mobility of ions with increase in temperature. The Kraft temperature increases from14 to 30 to $44^0$C, when the head group polarity of gemini surfactant increases from 12-4-12 DMA to 12-4-12 MEA to 12-4-12 DEA, respectively.

**Table 2.1** Kraft temperatures of a series of cationic surfactants

| Surfactants | Kraft temp., $k_T$ (°C) |
|---|---|
| 12-4-12 DMA | 14 |
| 12-4-12 MEA | 30 |
| 12-4-12 DEA | 44 |
| $C_{12}$TMAB | < 0 |
| $C_{12}$DMEAB | < 0 |
| $C_{12}$DEMAB | < 0 |

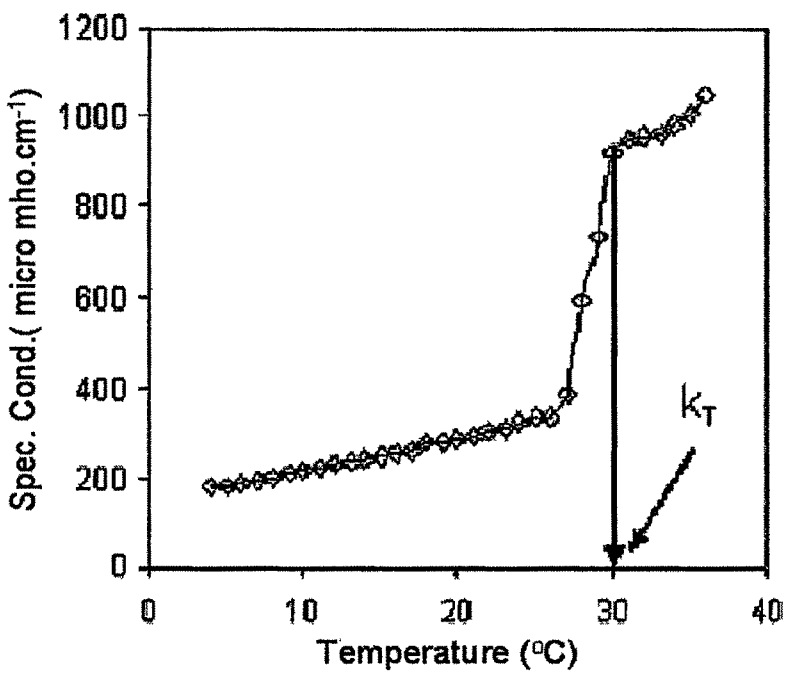


**Figure 2.1** Representative plot for determination of Kraft temperature for 12-4-12 MEA surfactant (1% w/v solution)

This can be explained in terms of effect of binding of counterion and head group polarity on micellization and hence on kraft temperature. It has been reported that increase in hydrophobic alkyl chain length of surfactant molecules assists in micellization. It is also reported that increase in hydrophobic alkyl chain of m-s-m type cationic surfactant increases kraft temperature [50]. This means increase in micellization tendency is related to kraft temperature. Binding of counterion which usually increases with increase in head group polarity of gemini surfactant (Table 2.2) would also enhance micellization and hence Kraft temperature.

### 2.3.2 Critical micelle concentration by conductometrically

It is well known that the conductance of surfactant solution changes with concentration at different rates below and above CMC. Premicellar aggregation of gemini surfactants has been observed to depend on spacer chain length by Zana [34]. He has reported that surfactant with spacer length (s) $\leq$ 10 does not show premicellar aggregates. The surfactants under study have 4 methylene unit spacer and hence are not expected to show premicellar aggregates. Surfactants were observed to dissociate completely at very low concentration and their conductance increases linearly with an increase in concentration up to CMC. Although the conductance continues to increase beyond CMC, the rate of increase in conductance is lower compared to that below CMC (Figure 2.2 & 2.4). This may be due to binding of some of the counterions to the micelles above CMC, causing a reduction in the effective charge on the micelles. The effect of variation in head group polarity of butane-1,4-bis(dodecyldimethylammonium bromide) surfactant on critical micellar concentration, binding of counterions to the micelles (β) and thermodynamic parameters of micellization was studied through conductance measurements at different temperatures. The results obtained are given in Table 2.2 and 2.4. The CMC values were observed to decrease from 1.5 x $10^{-3}$ to 8.1 x $10^{-6}$ M for the surfactants with higher polarity such as 12-4-12 DMA to 12-4-12 MEA to 12-4-12 DEA. This can be attributed to increase in terminal hydrophilicity and polarity of

surfactant molecule. Similar observation was made by Wettig et al [41] for cationic gemini surfactants with hydroxyl substituted polymethylene spacers.

The observed increase in binding of counterions (β) and decrease in average degree of micellar ionization (α) with increased head group polarity can be attributed to the increase in the polarizability and surface charge density of micelle, due to prominent negative inductive effect of $-C_2H_4OH$ groups and possible intra/inter molecular hydrogen bonding. Similar effect has been reported for conventional monomeric surfactants by Rosen and Song [51]. Similar trend in binding of counterions was also observed in SANS study of these surfactants. Influence of head group polarity on micellar parameters such as CMC, $\alpha_{ave}$ and β for monomeric surfactant was also studied for comparison and results are compiled in Table 2.2. The influence of head group polarity on micellar parameters was observed to be more pronounced in gemini surfactants than that in monomeric surfactants.

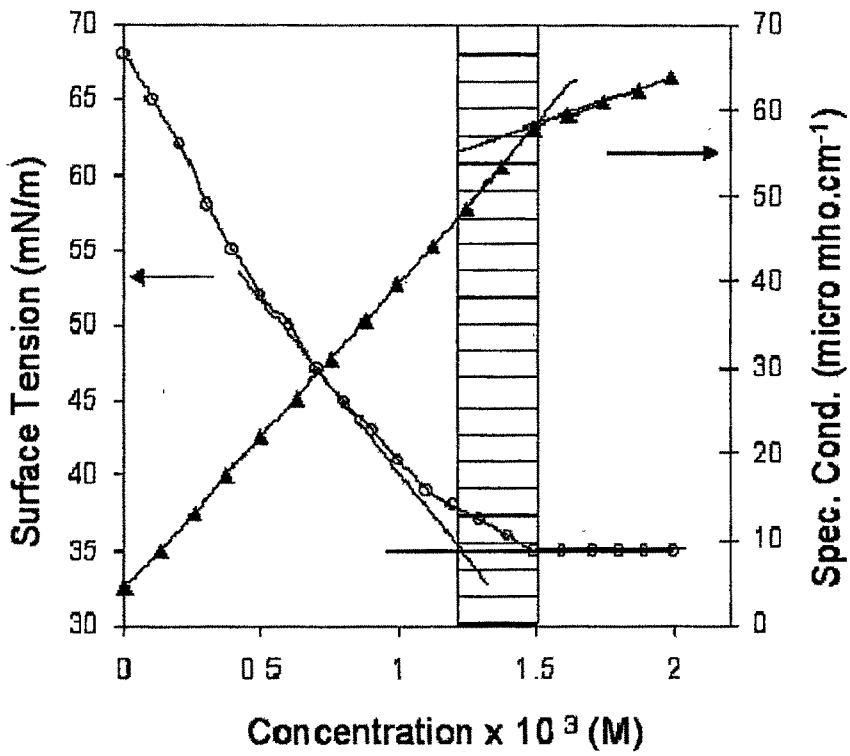


**Figure2.2 (a)** Critical micellar concentration of bis-cationic surfactant 12-4-12 DMA at 30 ± 0.1°C.
By conductance (▲), By surface tension (o).

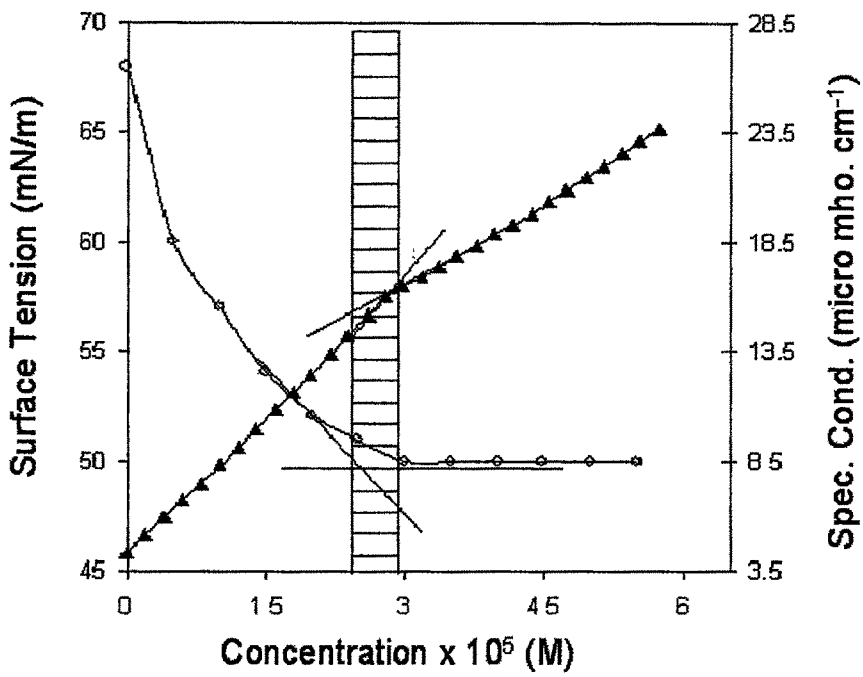


**Figure 2.2 (b)** Critical micellar concentration of bis-cationic surfactant 12-4-2 MEA at 30 ± 0.1°C.
By conductance (▲), By surface tension (o).

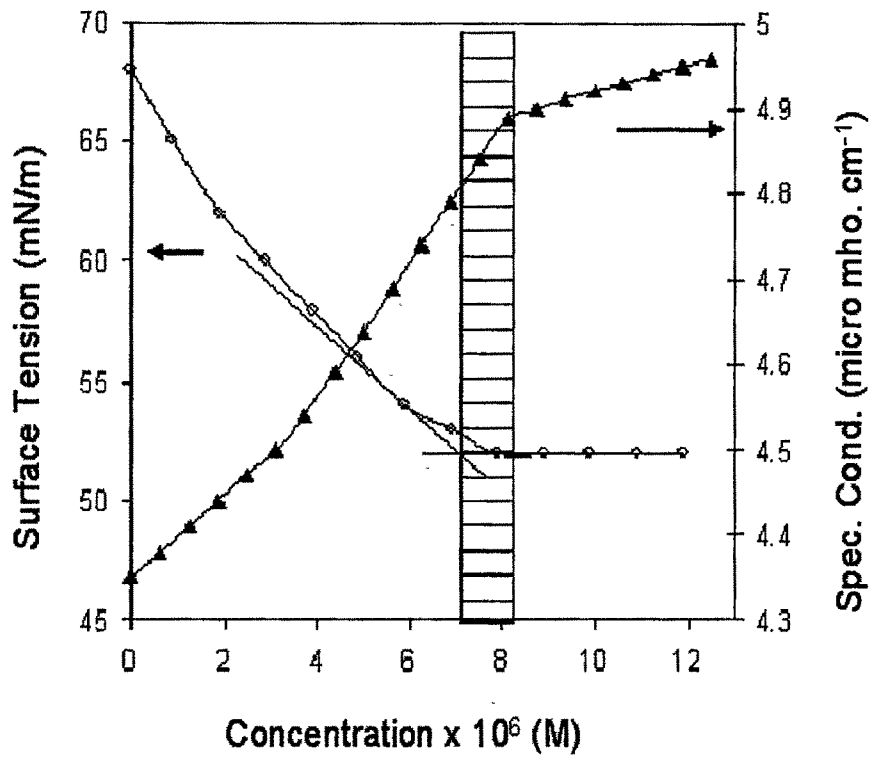


**Figure2.2 (c)** Critical micellar concentration of bis-cationic surfactant 12-4-12 DEA at 30 ± 0.1$^0$C.

By conductance (▲), By surface tension (o).

**Table 2.2** Effect of head group polarity and temperature on micellization parameters of bis-cationic surfactants and their monomeric counterpart.

| Surfactant system | Temperature ($^0$C.) | Critical micellar concentration CMC (M) | Average degree of micelle ionization $\alpha_{ave}$ | Binding of counterion ($\beta = 1 - \alpha_{ave}$) |
|---|---|---|---|---|
| 12-4-12 DMA | 30 | $1.5\pm0.1 \times 10^{-3}$ | 0.32 | 0.68 |
| | 35 | $1.6\pm0.1 \times 10^{-3}$ | 0.35 | 0.65 |
| | 40 | $1.9\pm0.1 \times 10^{-3}$ | 0.38 | 0.62 |
| | 45 | $1.9\pm0.1 \times 10^{-3}$ | 0.41 | 0.59 |
| | 50 | $2.1\pm0.1 \times 10^{-3}$ | 0.54 | 0.46 |
| 12-4-12 MEA | 30 | $2.8\pm0.1 \times 10^{-5}$ | 0.26 | 0.74 |
| | 35 | $2.9\pm0.1 \times 10^{-5}$ | 0.30 | 0.70 |
| | 40 | $3.4\pm0.1 \times 10^{-5}$ | 0.34 | 0.66 |
| | 45 | $3.6\pm0.1 \times 10^{-5}$ | 0.37 | 0.63 |
| | 50 | $3.8\pm0.1 \times 10^{-5}$ | 0.39 | 0.61 |
| 12-4-12 DEA | 30 | $8.1\pm0.1 \times 10^{-6}$ | 0.20 | 0.80 |
| | 35 | $8.7\pm0.1 \times 10^{-6}$ | 0.20 | 0.80 |
| | 40 | $9.9\pm0.1 \times 10^{-6}$ | 0.27 | 0.73 |
| | 45 | $10.6\pm0.1 \times 10^{-6}$ | 0.33 | 0.67 |
| | 50 | $11.2\pm0.1 \times 10^{-6}$ | 0.37 | 0.63 |
| $C_{12}$TMAB | 30 | $1.8\pm0.1 \times 10^{-2}$ | 0.34 | 0.66 |
| $C_{12}$DMEAB | 30 | $1.6\pm0.1 \times 10^{-2}$ | 0.32 | 0.68 |
| $C_{12}$DEMAB | 30 | $1.4\pm0.1 \times 10^{-2}$ | 0.31 | 0.69 |

### 2.3.3 Critical micellar concentration by spectrophotometrically

Use of dye in the determination of CMC is extensively reported. Dyes such as merocyanine, eosin, bromophenol blue, rhodamine and sudan are known to show a shift in the wavelength ($\lambda_{max}$) in the presence of micelles [52-54]. CMC values for a series of cationic gemini surfactant under study were measured by this method as a function of head group polarity and are given in Table 2.3. Bromophenol blue in water shows $\lambda_{max}$ at 590 nm and in the presence of surfactant shows $\lambda_{max}$ at 600 nm. Increasing surfactant concentration, gradually decrease the absorbance at 590 nm and increased absorbance at 600 nm. This implies that cationic surfactant may react with anionic dye to form an surfactant-dye ion association complex. The $\lambda_{max}$ of dye in micellar medium is sufficiently different from the $\lambda_{max}$ of dye in aqueous medium. The absorbance at 590 nm can be followed as a function of surfactant concentration to measure the extent of dye uptake from solution as shown in Figure 2.3(a, b, c). The decrease in absorbance at 590 nm is plotted as a function of increase in surfactant concentration as shown in Figure 2.3 (a, b, c). At lower concentration decrease of absorbance is small, whereas at near CMC the decrease of absorbance is sharp. At this point absorbance varies strongly over a range of surfactant concentration, depleting that the most of dye molecules are associated with surfactant molecules. At high enough surfactant concentration the absorbance vs concentration curve will again flatten. The two linear lines are plotted and intersect at point shown in Figure 2.3 (a, b, c) is defined as the CMC. CMC values measured by this technique are in good agreement with CMC by conductance and surface tension measurement (Table 2.3).

**Table 2.3** Critical micelle concentration of a series of bis-cationic surfactant

| Surfactant system | CMC by Conductance (M) | CMC by Dye adsorption (M) | CMC by Surface tension (M) |
|---|---|---|---|
| 12-4-12 DMA | $1.5 \pm 0.1 \times 10^{-3}$ | $1.4 \pm 0.1 \times 10^{-3}$ | $1.3 \pm 0.1 \times 10^{-3}$ |
| 12-4-12 MEA | $2.8 \pm 0.1 \times 10^{-5}$ | $2.8 \pm 0.1 \times 10^{-5}$ | $2.7 \pm 0.1 \times 10^{-5}$ |
| 12-4-12 DEA | $8.1 \pm 0.1 \times 10^{-6}$ | $8.0 \pm 0.1 \times 10^{-6}$ | $7.9 \pm 0.1 \times 10^{-6}$ |

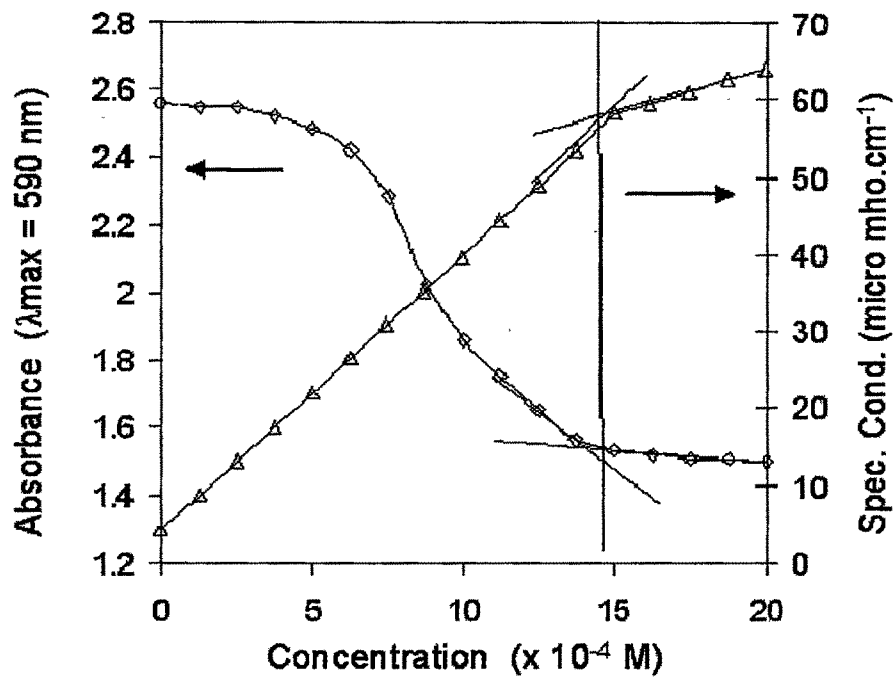


**Figure 2.3(a)** Critical micelle concentration of bis-cationic surfactant 12-4-12 DMA at 30 ± 0.1°C.

By conductance (△), By UV-visible spectroscopy (◇).

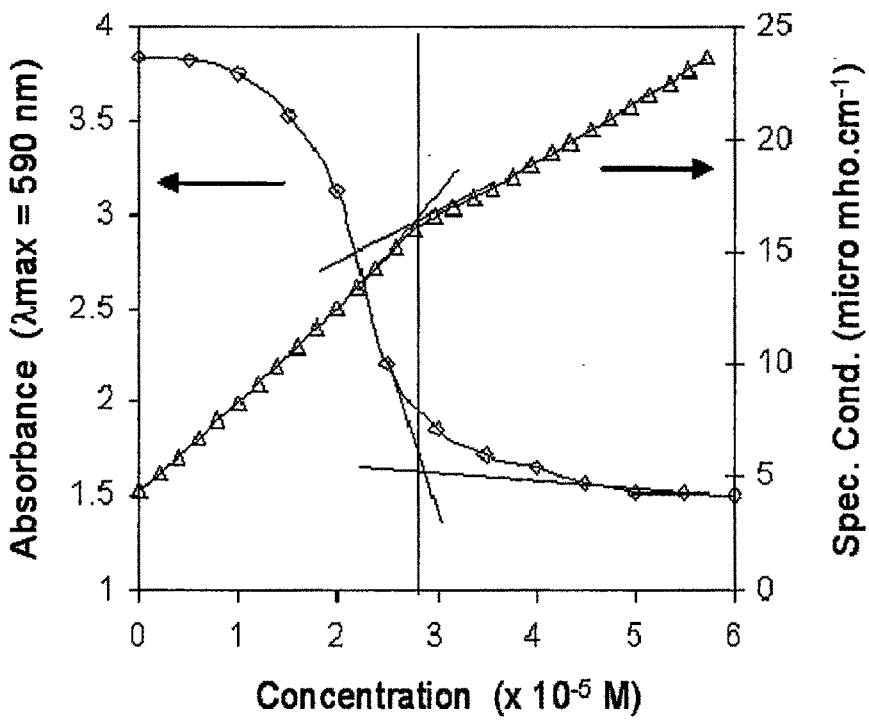


**Figure 2.3(b)** Critical micellar concentration of bis-cationic surfactant 12-4-12 MEA at 30 ± 0.1$^0$C.

By conductance (△), By UV-visible spectroscopy (◇).

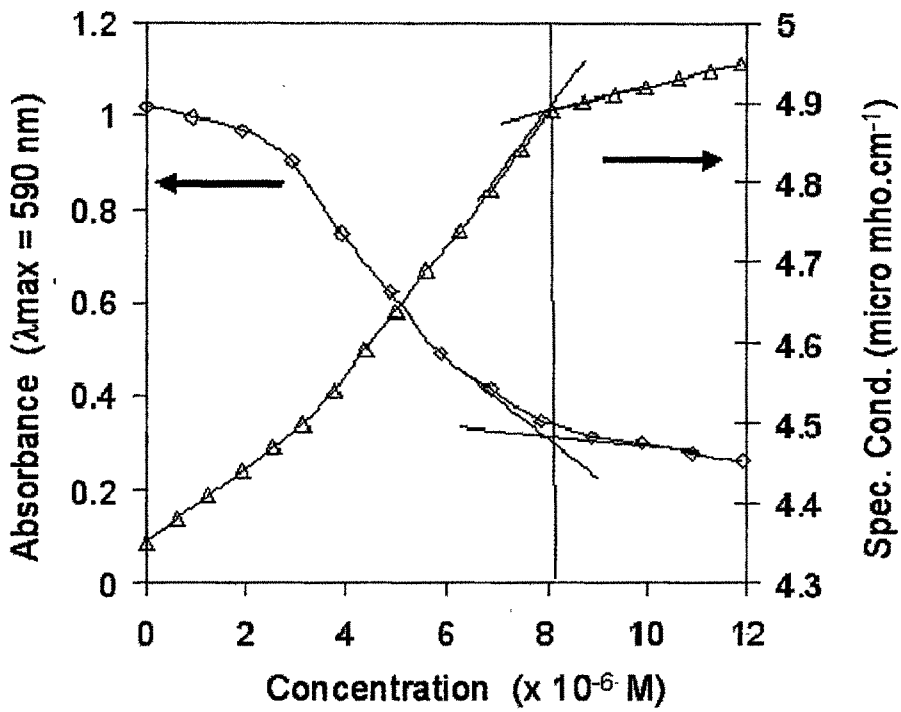


**Figure 2.3(c)** Critical micellar concentration of bis-cationic surfactant 12-4-12 DEA at 30 ± 0.1$^0$C.

By conductance (△),By UV-visible spectroscopy (◇).

### 2.3.4 Thermodynamic Parameters of Micellization

The mass action model was applied to compute thermodynamic parameters of micellization. This model has been reported to explain experimental data particularly well for ionic micelles [55]. The standard Gibbs-free energy change involved in the aggregation of bis-cationic surfactants into partially ionized micelles in aqueous solution is given as [55,56]

$$\Delta G^{\circ}_{m} = RT\,(1.5 - \alpha_{ave})\,\ln CMC \qquad (1)$$

The enthalpy change and entropy change for the micellization process can be determined using Gibbs- Helmholtz equation for aqueous solutions,

$$\Delta H^{\circ}_{m} = -\,RT^{2}(1.5 - \alpha_{ave})d\ln CMC/dT \qquad (2)$$

and

$$\Delta S^{\circ}_{m} = \frac{\Delta H^{\circ}_{m} - \Delta G^{\circ}_{m}}{T} \qquad (3)$$

Where R, T, and $\alpha_{ave}$ are gas constant, absolute temperature and average degree of micellar ionization respectively.

The thermodynamic parameters of micellization derived from conductance data at different temperatures (Figure 2.4) for surfactants under study are compiled in Table 2.4. The observed more negative Gibb's free energy of micellization for the surfactants with increasing head polarity indicates favored micellization. Negative values of enthalpy ($\Delta H^{\circ}_{m}$) of micellization indicate exothermic nature of micellization process. Nusselder and Engbert's [57] have suggested that for the negative $\Delta H^{\circ}_{m}$, the dispersion forces play major role in the micelle formation. Also, the observed exothermicity can be attributed to possible surfactant-solvent

interactions. The enthalpy values do not vary significantly with temperature, indicating no significant variation in the environment surrounding the hydrocarbon chain of the surfactant molecule with temperature. The entropy of micellization ($\Delta S^{o}_{m}$) being more positive, in the system under study, micellization is entropy ($\Delta S^{o}_{m}$) driven. The more positive values of entropy may be due to the breaking of bulk water structure around the molecules. This leads to more disorder in the structure of water and favors the micellization at lower concentration. More positive entropy values indicate micellization process to be more spontaneous. High entropy changes are generally associated with a phase change. Hence it can be assumed that the micelles form separate phase in these systems. The observed sharp increase in the entropy values indicates that increasing head group polarity favors micellization process (Table 2.4).

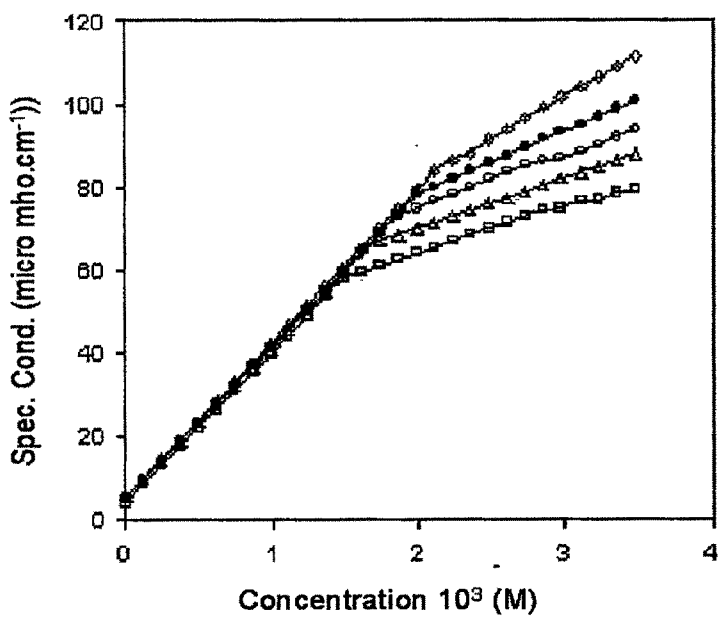


**Figure 2.4** **(a)** Effect of temperature on 12-4-12 DMA bis-cationic surfactant, 30 (□), 35 (Δ), 40 (o), 45 (•) and 50 $^{0}$C(◇)

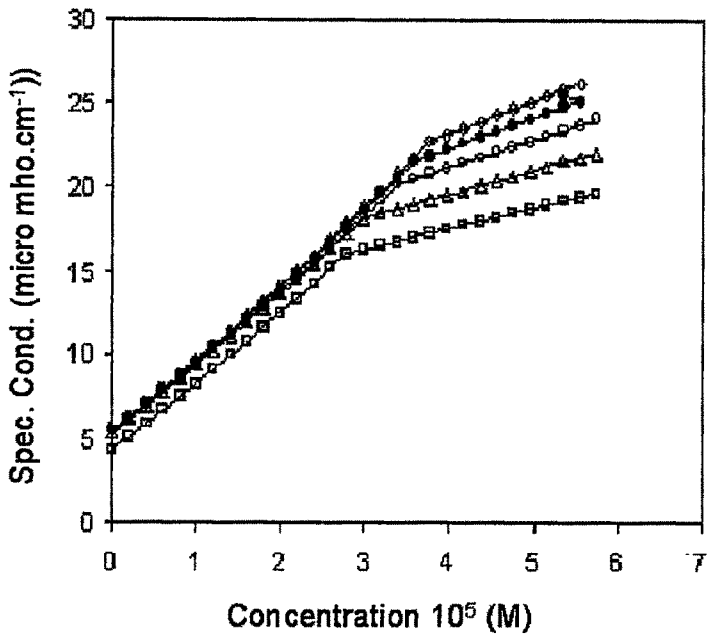


**Figure 2.4 (b)** Effect of temperature on 12-4-12 MEA bis-cationic surfactant, 30 (□), 35 (Δ),40 (o),45 (●) and 50 $^0$C(◇)

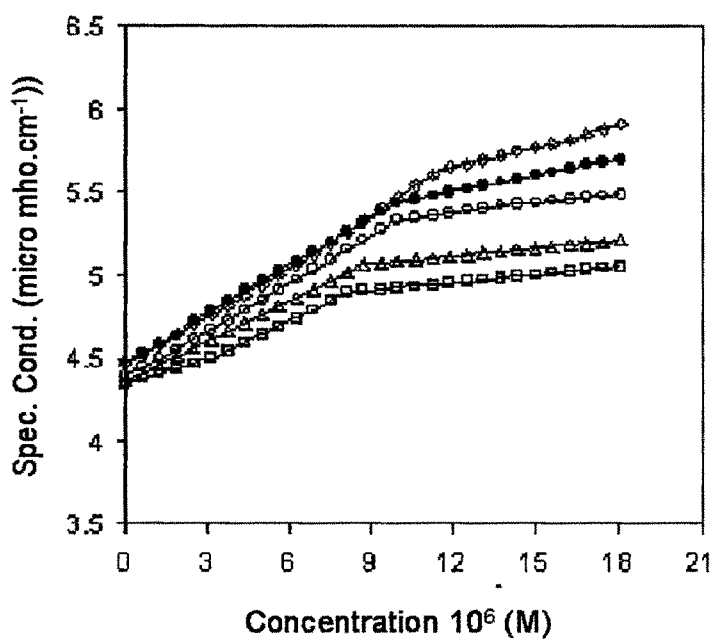


**Figure 2.4 (c)** Effect of temperature on 12-4-12 DEA bis-cationic surfactant, 30 (□), 35 (Δ), 40 (o), 45 (●) and 50 $^0$C(◇)

**Table 2.4** Effect of head group polarity and temperature on thermodynamic parameters of micellization of bis-cationic surfactants

| Surfactant system | Temperature (°C.) | Gibb's Free energy ($-\Delta G^{\circ}_{m}$) $KJmol^{-1}$ | Enthalpy ($-\Delta H^{\circ}_{m}$) $KJmol^{-1}$ | Entropy ($\Delta S^{\circ}_{m}$) $Jk^{-1}mol^{-1}$ |
|---|---|---|---|---|
| 12-4-12 DMA | 30 | 19.34 ±1.3 | 16.21± 0.9 | 10.32 ±1.1 |
| | 35 | 18.92 ±1.3 | 16.33 ±0.9 | 8.42 ±1.1 |
| | 40 | 18.31 ±1.4 | 16.42 ±0.9 | 6.04 ±1.1 |
| | 45 | 17.92 ±1.4 | 16.50 ±0.9 | 4.48 ±1.1 |
| | 50 | 15.88 ± 1.3 | 15.61 ±0.9 | 0.81 ±1.1 |
| 12-4-12 MEA | 30 | 32.77 ±1.5 | 14.96 ±0.9 | 58.78 ±1.2 |
| | 35 | 32.01 ±1.5 | 14.95 ±0.9 | 55.39 ±1.2 |
| | 40 | 31.05 ±1.5 | 14.93 ±0.9 | 51.50 ±1.2 |
| | 45 | 30.59 ±1.5 | 15.01 ±0.9 | 48.99 ±1.2 |
| | 50 | 30.36 ±1.5 | 15.21 ±0.9 | 46.88 ±1.2 |
| 12-4-12 DEA | 30 | 38.39 ±1.6 | 14.68 ±0.9 | 78.25 ±1.3 |
| | 35 | 38.77 ±1.6 | 15.27 ±0.9 | 76.30 ±1.3 |
| | 40 | 36.85 ±1.6 | 14.92 ±0.9 | 70.06 ±1.2 |
| | 45 | 35.42 ±1.6 | 14.65 ±0.9 | 65.31 ±1.2 |
| | 50 | 34.58 ±1.7 | 14.60 ±0.9 | 61.85 ±1.2 |

### 2.3.5 Critical Micelle Concentration and Surface Active Parameters

The surface tension measurement can be used to study the various surface phenomena or surface active parameters such as CMC, $\Gamma_{max}$, $A_{min}$, $\Pi$, and $\Delta G^{o}_{ad}$ of surfactant system. The surface saturation $\Gamma_{max}$, can be used as a measure of maximum extent of adsorption of surfactant at the air/water interface and can be calculated by using Gibb's adsorption equation [58, 59] for dilute solutions.

$$\Gamma_{max} = -1/RT(d\gamma/d\ lnC) \qquad (4)$$

where $\Gamma_{max}$, $\gamma$ and C are surface excess concentration, surface tension and concentration respectively. From the surface excess values it is possible to calculate minimum area per molecule ($A_{min}$) in angstroms square at air/water interface using relation [60],

$$A_{min} = 10^{16}/N_A\Gamma_{max} \qquad (5)$$

where $N_A$ is Avogadro's number.

The surface excess concentration values ($\Gamma_{max}$) were observed to decrease and $A_{min}$ values were observed to increase when head group polarity of bis-cationic surfactants increased from 12-4-12 DMA to 12-4-12 MEA to 12-4-12 DEA (Table 2.5). The effectiveness of a surfactant molecule is measured by $CMC/C_{10}$ and surface pressure value ($\Pi$). The surface pressure at the CMC is given as $\gamma_{CMC} = \gamma_w - \gamma_{CMC}$, where $\gamma_w$ and $\gamma_{CMC}$, are the surface tension of pure water and the surface tension at CMC, $C_{10}$ is the concentration of surfactant required to reduce the surface tension of pure water by 10 mN/m units. The $CMC/C_{10}$ and surface pressure value ($\Pi_{CMC}$) were observed to decrease with increase in head group polarity (Table 2.5), indicating that the increase in head group polarity of bis-cationic surfactant decreases the adsorption efficiency of surfactant molecule.

The Gibb's free energy change of adsorption ($\Delta G^{\circ}_{ad}$) was calculated by using equation (6) and is given in Table 2.5.

$$\Delta G^{\circ}_{ad} = RT\ln CMC - N_A \Pi_{CMC}. A_{min} \qquad (6)$$

The $\Delta G^{\circ}_{ad}$ values are more negative than their corresponding $\Delta G^{\circ}_{m}$ values indicating that when a micelle is formed, work has to be done to transfer the surfactant molecules from the surface to the micelle through aqueous medium [27]. The difference between the $\Delta G^{\circ}_{ad}$ and $\Delta G^{\circ}_{m}$ values is called as effective Gibb's free energy change of micellization ($\Delta G^{\circ}_{eff}$) and is given in Table 2.5. It was observed to decrease with increase in head group polarity, indicating minimum energy barrier between the adsorption and micellization phenomenon. This is also in agreement with the results obtained for $CMC/C_{10}$ and surface pressure values ($\Pi_{CMC}$).

**Table2.5.** Critical micelle concentration (CMC), CMC/$C_{10}$, surface pressure ($\Pi_{CMC}$), surface excess concentration ($\Gamma_{max}$), minimum area per molecule at air/water interface ($A_{min}$) and Gibb's free energy of adsorption ($\Delta G^{o}_{ad}$) and effective Gibb's free energy ($\Delta G^{o}_{eff}$) of bis-cationic surfactant as function of head group polarity at 30±0.1°C.

| Surfactant systems | CMC (M) | $A_{min}$ ($Å^2$) | $\Gamma_{max}$ x $10^{10}$ mol.cm$^{-2}$ | $\Pi_{CMC}$ mN/m | $\Delta G^{o}_{eff}$ KJmol$^{-1}$ | - $\Delta G^{o}_{ad}$ KJmol$^{-1}$ | CMC/$C_{10}$ |
|---|---|---|---|---|---|---|---|
| 12-4-12 DMA | 1.3±0.2 x $10^{-3}$ | 83.6 | 1.99 ± 0.1 | 33 | 14.8±1.5 | 34.1 ±1.5 | 4.6 |
| 12-4-12 MEA | 2.7 +0.2 x $10^{-5}$ | 155 | 1.08 ± 0.1 | 18 | 10.5±1.5 | 43.3 ±1.5 | 3.7 |
| 12-4-12 DEA | 7.9 ±0.2 x $10^{-6}$ | 163 | 1.02 ± 0.1 | 16 | 6.9 ±1.5 | 45.3 ±1.5 | 2.0 |

### 2.3.6 Intrinsic Viscosity and Hydration of Micelle

The plot of reduced viscosity of aqueous surfactant solutions against concentration at different temperatures for surfactants with variable head polarity i.e.12-4-12 DMA, MEA and DEA are given in Figure 2.5. The concentration dependence of viscosity can also be analyzed in terms of intrinsic viscosity. It is a function of shape and size of particle present in the solution and also of solute-solvent interaction [61] From intrinsic viscosity the hydration of micelles ($h_m$) in $cm^3g^{-1}$ is obtained through the extension of the Einstein equation [62-65].

$$\eta = 2.5 (V_s + h_m) \qquad (7)$$

$$\eta = \nu(V_s + h_m V_s^o) \qquad (8)$$

where $V_s$ ($cm^3g^{-1}$) is partial specific volume of micelles, $h_m$ is the hydration of micelles, $\eta$ is the intrinsic viscosity and micelles are assumed to be spherical with shape factor ($\nu$) of Einstein coefficient equal to 2.5. The partial specific volume ($V_s$) of micelle was calculated from slope of the linear plots obtained by the equation $\rho = \rho_o + (1- Vs\ \rho_o)C$, where $\rho$ is the density of solution at given concentration (C) and $\rho_o$ is the density of water. The estimated values of $\eta$, $V_s$, $h_m$ and $\nu$ at different temperatures for each surfactant are given in Table 2.6. Intrinsic viscosity ($\eta$) of micellar solution and hydration of micelle ($h_m$) were observed to increase with increase in head polarity and decrease with increase in temperature.

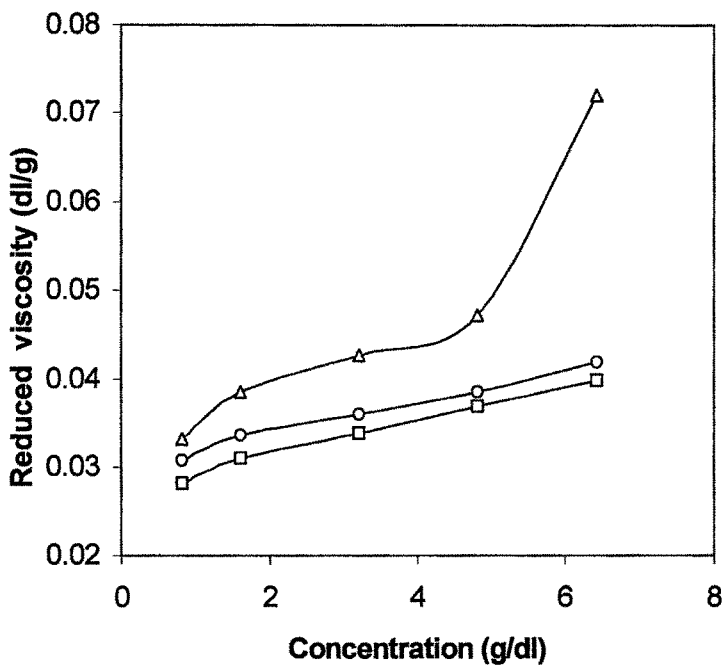


**Figure 2.5 (a)** Effect of temperature on reduced viscosity of 12-4-12 DMA 30 (Δ), 40 (o) and 50 °C(□).

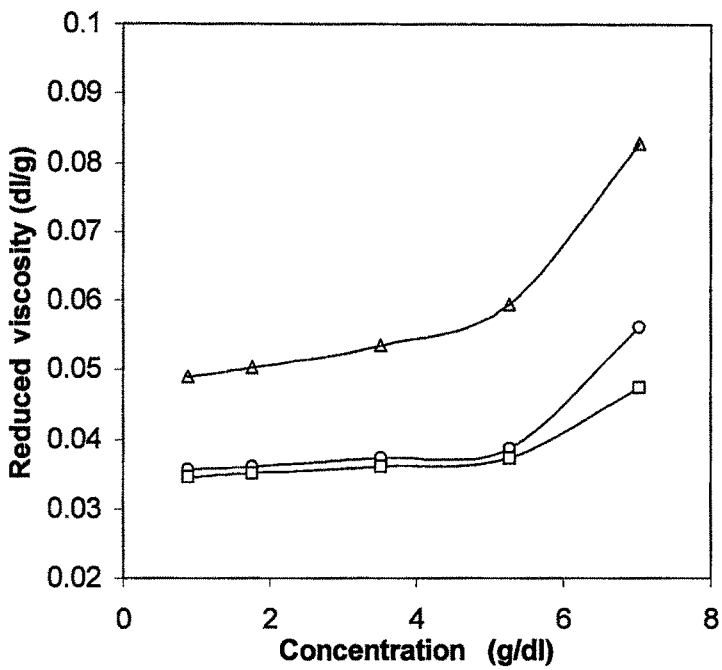


**Figure 2.5 (b)** Effect of temperature on reduced viscosity of 12-4-12 MEA 30 (Δ), 40 (o) and 50 °C(□).

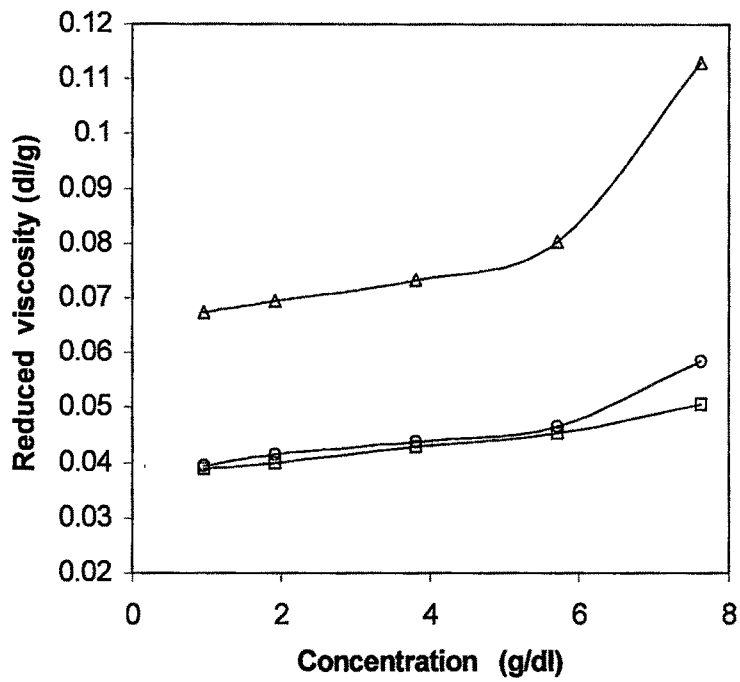


**Figure 2.5 (c)** Effect of temperature on reduced viscosity of 12-4-12 DEA 30 (Δ), 40 (o) and 50 °C(□).

**Table 2.6** Effect of head polarity and temperature on intrinsic viscosity, partial specific volume, hydration and shape factor of micelle.

| Surfactant system | Temperature (°C.) | Intrinsic viscosity (η) dl/g | Partial specific volume (Vs) $cm^3/g$ | Hydration of micelles ($h_m$) $cm^3/g$ | Shape factor (ν = η/Vs) | The axial ratio from SANS (b/a) |
|---|---|---|---|---|---|---|
| 12-4-12 DMA | 30 | 0.0365 | 0.9784 | 0.134 | 3.7 | 3.5 |
| | 40 | 0.0301 | 0.9846 | 0.119 | 3.1 | --- |
| | 50 | 0.0283 | 0.9914 | 0.025 | 2.9 | 2.8 |
| 12-4-12 MEA | 30 | 0.0462 | 0.9361 | 0.912 | 4.9 | 4.2 |
| | 40 | 0.0350 | 0.9483 | 0.452 | 3.7 | --- |
| | 50 | 0.0340 | 0.9578 | 0.402 | 3.5 | 3.2 |
| 12-4-12 DEA | 30 | 0.0643 | 0.9117 | 1.660 | 7.1 | --- |
| | 40 | 0.0383 | 0.9168 | 0.603 | 4.2 | --- |
| | 50 | 0.0374 | 0.9224 | 0.558 | 4.1 | 3.7 |

The shape factors (ν) for bis-cationic surfactants were calculated by using equation (8) and are given in Table 2.6. Shape factor (ν) was observed to increase from 3.7 to 4.9 to 7.1 with head group polarity of bis-cationic surfactant on successive replacement of methyl group by ethanolic group at quaternary amine heads of the surfactant. This data is consistent with the data obtained from SANS analysis for micellar dimension (b/a) as shown in Table 2.6. The shape and size of micelles was also observed to be sensitive towards temperature variations.

### 2.3.7 Aggregation Behavior Through SANS Measurement

In SANS experiment a beam of neutron is directed upon the sample under examination and neutron scattering intensities in different directions are measured. Since neutron is scattered by nuclei in sample, even isotopes of the same element can differ in their scattering power. Thus by taking aggregates in $D_2O$ rather than in $H_2O$, the scattering intensities of various regions can be obtained, since deuteron and protons differ widely in their respective scattering intensities.

#### Data Analysis

In SANS one measures the differential scattering cross-section per unit volume ($d\Sigma/d\Omega$) as a function of scattering vector Q. For a system of charged interacting micelles $d\Sigma/d\Omega$ is given by [47, 48, 66].

$$\frac{d\Sigma}{d\Omega} = n(\rho_m - \rho_s)^2 V^2 \left[\left\langle F(Q)^2 \right\rangle + \left\langle F(Q) \right\rangle^2 \left(S(Q) - 1\right)\right] + B \qquad (9)$$

where n denotes the number density of the micelles, $\rho_m$ and $\rho_s$ are respectively the scattering length densities of the micelles and the solvent and V is the volume of the micelle. The aggregation number N of the micelle is related to the micelle volume V by the relation V = Nv, where v is the volume of the surfactant monomer. F(Q) is the single particle form factor and S(Q) is the interparticle structure factor. B is a constant term that represents the incoherent scattering background, which

is mainly due to hydrogen in the sample. The single particle form factor has been calculated by treating the micelle as prolate ellipsoidal [66]. The prolate ellipsoidal shape (a = c ≠ b) of the micelles is widely used in the analysis of SANS data because it also represents the other different possible shapes of the micelles such as spherical (a = b = c) and rod-like (b >> a). For such an ellipsoidal micelle

$$\langle F(Q)^2 \rangle = {}_0\int^1 [F(Q,\mu)^2 d\mu \,] \qquad (10)$$

$$\langle F(Q) \rangle^2 = {}_0\int^1 [F(Q,\mu) d\mu \,]^2 \qquad (11)$$

$$F(Q,\mu) = 3(\sin\omega - \omega\cos\omega) / \omega^3 \qquad (12)$$

$$\omega = Q[a^2(1-\mu^2) + b^2\mu^2]^{1/2} \qquad (13)$$

where a and b are respectively the semi minor and semi major axes of the ellipsoidal micelle and $\mu$ is the cosine of the angle between the axis of resolution and the wave vector transfer Q.

In general, micellar solutions of ionic surfactants show a correlation peak in the SANS distribution [49]. The peak arises because of the interparticle structure factor S(Q) and indicates the presence of electrostatic interactions between the micelles. S(Q) specifies the correlation between the centers of different micelles and it is Fourier transform of the radial distribution function g(r) for the mass centers of the micelle. We have calculated S(Q) as derived by Hayter and Penfold model [66] from the Ornstein-Zernike equation and using the rescaled mean spherical approximation. The micelle is assumed to be a rigid equivalent sphere of diameter $\sigma = 2(a^2b)^{1/3}$ interacting through a screened Coulomb potential, which is given by

$$u(r) = u_0\sigma\frac{\exp[-\kappa(r-\sigma)]}{r}, \quad r > \sigma \qquad (14)$$

where r is inter-ionic centre to centre distance and $\kappa$ is the Debye-Hückel inverse screening length and is calculated by

$$\kappa = \left[ \frac{8\pi N_A e^2 I}{10^3 \varepsilon k_B T} \right]^{1/2} \qquad (15)$$

where I is the ionic strength of the micellar solution and is determined by the CMC and dissociated counterions from the micelles. The fractional charge ($\alpha$) per surfactant molecule in the micelles is given as $\alpha$ = Z/N, where Z is the micellar charge. The contact potential $u_0$ is given by

$$u_0 = \frac{Z^2 e^2}{\pi\varepsilon \ \varepsilon_0 \sigma (2 + \kappa \ \sigma)^2} \qquad (16)$$

where $\varepsilon$ is the dielectric constant of the solvent medium, $\varepsilon_0$ is the permittivity of free space and *e* is the electronic charge.

Although micelles may produce polydisperse systems, we have assumed them as monodisperse for the simplicity of the calculation and to limit the number of unknown parameters in the analysis. The dimensions of the micelle (b/a), aggregation number (N) and the fractional charge ($\alpha$) have been determined from the analysis. The semimajor axis (b), semiminor axis (a = c) and the fractional charge ($\alpha$) are the parameters used in analyzing the SANS data. The aggregation number is calculated from the relation $N = 4\pi a^2 b/3v$, where v is the volume of the surfactant monomer. The prameters in the analysis were optimized by means of nonlinear least-square fitting program.

### *Effect of head group polarity*

Effect of head group polarity of cationic surfactants on aggregation behavior was studied through SANS. The 100 mM aqueous solution of 12-4-12 DEA was highly viscous and hazy at 30 °C, because of its Kraft temperature of 44°C. Hence SANS experiments were carried out at 50 °C for all 12-4-12 DMA/MEA/DEA (Figure 2.6) and at 30°C for 12-4-12 DMA/MEA, at 100 mM concentration. Also SANS experiment were carried out for their monomeric counterparts $C_{12}$TMAB, $C_{12}$EDMAB and $C_{12}$DEMAB surfactants at 30°C and 200 mM concentration (Figure 2.7). All SANS distributions show well defined correlation peaks because of interparticle structure factor S(Q). The correlation peaks appeared at around $Q_{max} \simeq 2\pi/D$ where D is the average distance between the micelle. Since $Q_{max}$ was observed to vary with the head group polarity one can state that the number density (n) of micelles varies with head group polarity. From figure 2.6 a slight shift in the peak position towards higher Q values with decreased scattering intensities is observed with decrease in head group polarity of surfactants from 12-4-12 DEA to 12-4-12 MEA to 12-4-12 DMA. The extracted micellar parameters from SANS data are given in Table 2.7. From the results the aggregation number (N) was observed to increase from 60 to 75 and the effective fractional charge was observed to decrease from 0.18 to 0.14 when the head group polarity increased. These results indicate that the increased head group polarity of cationic gemini favoured micellar growth along the semi-major axis (b) as shown in Table 2.7. As seen from the results in Table 2.7, the influence of head group polarity on micellar growth is more pronounced at 30°C than at 50°C. This can be rationalised by the possible breaking of inter/intra molecular H-bonding at higher temperature, which can be supported by the observed opposite trend in the equilibrium distance between charged heads (d) as a function of head group polarity at 30 and 50 °C as shown in Table 2.7. No shift in peak position and no significant change in scattering intensity were observed in Figure 2.7 when head group polarity of monomeric surfactants increased from $C_{12}$TMAB to $C_{12}$DEMAB. The micellar

parameters for monomeric surfactants such as aggregation number (N), fractional charge (α) and dimension (b/a) of micelles are given in Table 2.8.

Table **2.7** Effect of head group polarity on micellar parameters of dimeric surfactants as determined from SANS at 100 mM and at 50°C,

| surfactant system | N | α | b (Å) | a (Å) | b/a | d (Å) |
|---|---|---|---|---|---|---|
| 12-4-12DMA | 60 (80) | 0.18 (0.16) | 47.8 ( 61.8) | 16.9 (17.2) | 2.82 (3.59) | 7.71 (7.42) |
| 12-4-12 MEA | 69 (108) | 0.16 (0.12) | 56.6 ( 78.6) | 17.5 (18.6) | 3.23 ( 4.23) | 7.88 (7.26) |
| 12-4-12 DEA | 75 | 0.14 | 64.8 | 17.8 | 3.64 | 7.96 |

N = aggregation number, α = fractional charge, a = semi-minor axis, b = semi-major axis and d = equilibrium distance between head groups.

(Note: The values given in parentheses are the micellar parameters obtained from SANS at 30 °C)

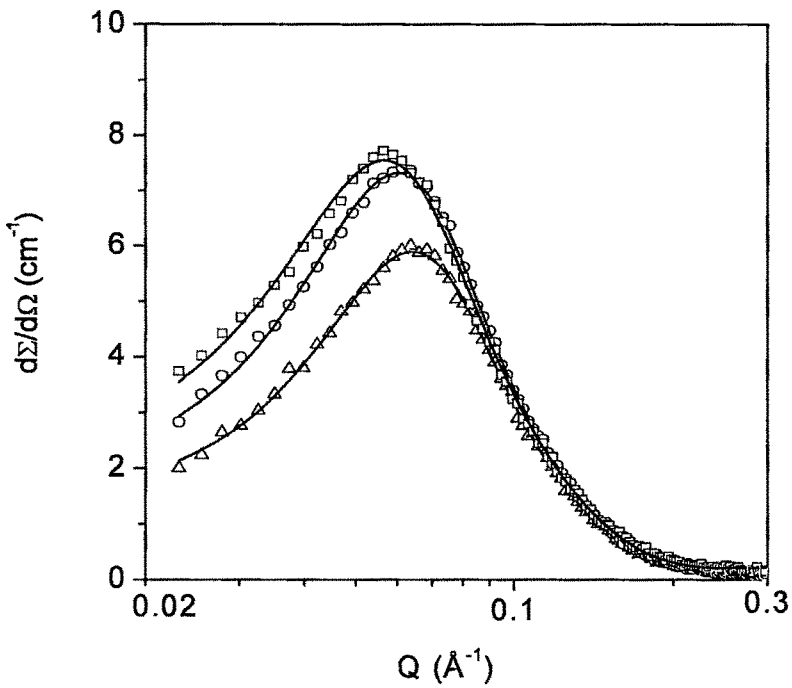


**Figure 2.6** SANS profil for 12-4-12 DMA/MEA/DEA at 100 mM and at 50°C. The solid line shows the theoretical fits and the symbols are experimentally determined values.
12-4-12 [DMA(Δ), MEA(O) and DEA(□)]

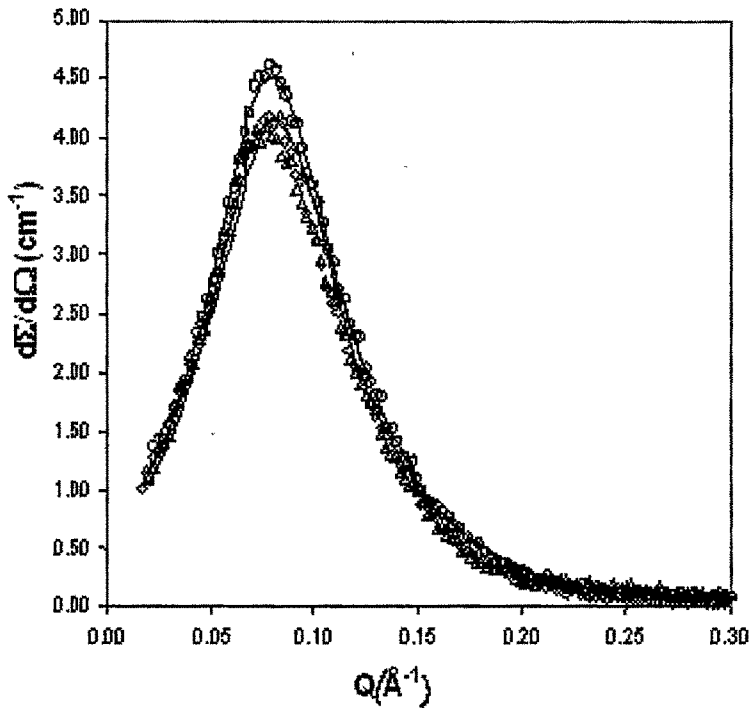


**Figure 2.7** SANS profil for $C_{12}$TMAB, $C_{12}$DMEAB, $C_{12}$DEAB at 200 mM and at 30 °C. The solid line shows the theoretical fits and the symbols are experimentally determined values

$C_{12}$TMAB (△), $C_{12}$DMEAB (◇), $C_{12}$DEAB (O).

**Table 2.8.** Effect of head group polarity of monomeric surfactants at 200 mM concentration and at 30°C

| Surfactant System | N | α | b (Å) | a (Å) | b/a | d (Å) |
|---|---|---|---|---|---|---|
| $C_{12}$TMAB | 69 | 0.15 | 31.2 | 15.4 | 2.0 | 8.3 |
| $C_{12}$DMEAB | 67 | 0.15 | 34.7 | 15.2 | 2.3 | 8.7 |
| $C_{12}$MDEAB | 67 | 0.16 | 37.9 | 15.5 | 2.4 | 9.0 |

N = aggregation number, α = fractional charge, a = semi-minor axis, b = semi-major axis, b/a =axial ratio and d = equilibrium distance between charged heads.

***Effect of surfactant concentration***

The SANS data from 12-4-12 MEA bis-cationic surfactant at different concentration and at 30°C is illustrated in Figure 2.8. The concentration range examined was 50 to 100 mM. It was observed that with increased concentration there is little shift in the peak position towards high Q value with overall increase in the peak intensity. With increase in concentration the distance between the micelles decreases indicating an increase in number density of micelles. The increase in concentration of surfactant helps aggregation growth along the direction of semi-major axis to forms more elongated ellipsoidal micelle (b/a = 4.2). The effective fractional charge was observed to decrease with increase in concentration of surfactants from 50 to 100 mM. This decrease in effective fractional charge with concentration is attributed to increase in aggregation number which increases the surface charge density on surface of micelle and helps to increase association of counterions (Table 2.9).

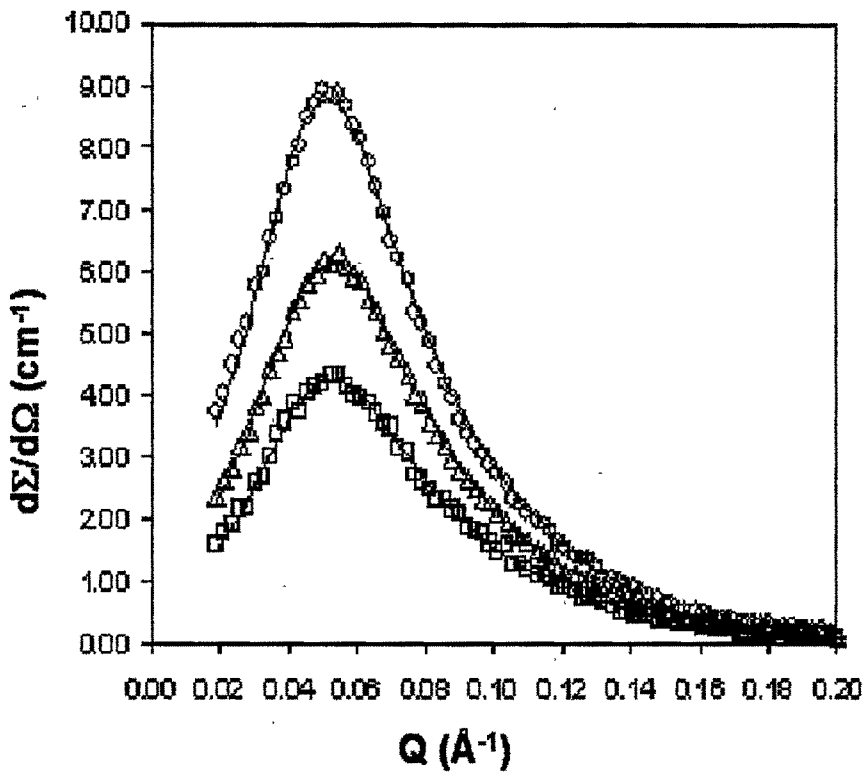


**Figure 2.8** Effect of variation of concentration on SANS distribution for 12-4-12 MEA bis-cationic surfactant at 30 °C.
100 mM (O), 75 mM (Δ) and 50 mM (□).

**Table 2.9** Effect of variation in concentration on micellar parameters of 12-4-12 MEA bis-cationic surfactant at 30 °C.

| concentrations (mM) | (N) | (α) | a (Å) | b (Å) | b/a |
|---|---|---|---|---|---|
| 100 | 108±8 | 0.11±0.01 | 18.6±0.5 | 78.6±1.8 | 4.23±0.05 |
| 75 | 81±6 | 0.14±0.01 | 18.3±0.5 | 60.8±1.5 | 3.34±0.05 |
| 50 | 63±5 | 0.17±0.01 | 17.7±0.5 | 50.4±1.4 | 2.78±0.06 |

N = aggregation number, α = fractional charge, a = semi-minor axis, b = semi-major axis, b/a = axial raio.

***Average equilibrium distance between two charged heads***

In aqueous solution two covalently connected positively charged head groups of a dimeric surfactant tend to maintain a critical distance between the charged heads to overcome Coulombic force of repulsion. We have estimated this equilibrium distance (d) from the SANS data assuming it to be equal to $(4\pi a_{eff}^2/N)^{1/2}$, where $a_{eff} = (a^2b)^{1/3}$, considering the micelles to be ellipsoidal. We have observed d ~ 8.32 Å for DTAB which is good agreement with the value reported by Zana [45]. Based on the similar approach the equilibrium distance between the charged heads calculated for the surfactants under study are given in Table 2.7 and 2.8. The equilibrium distance between the charged heads for gemini surfactant was observed to decrease with increase in head group polarity at 30°C. However, at 50°C, d was observed to increase with increasing head polarity. The observed decrease with head polarity at 30°C can be attributed to increased possibility of the inter/intra molecular hydrogen bonding at 30°C whereas at higher temperature these weaker bonds are likely to be disrupted and hence d was observed to increase with increase in head polarity at 50 °C.

### 2.3.8 Foamability and Foam Stability

Foamability and foam stability of 12-4-12 DMA surfactant as a function of increase in the number of $-C_2H_4OH$ groups at head group level was determined manually as per the method reported by Shah [46]. The results are given in Table 2.10. Foamability was observed to decrease and foam stability was observed to increase with increase in head group polarity from 12-4-12 DMA to 12-4-12 MEA to 12-4-12 DEA. This can be attributed to formation of more compact and stable micelles.

**Table 2.10** Effect of head group polarity on foamabilty and stability of bis-cationic surfactant.

| Surfactant system | Foamability ($cm^3$) | Foam stability (min.) |
|---|---|---|
| 12-4-12 DMA | 56 | 14 |
| 12-4-12 MEA | 25 | 34 |
| 12-4-12 DEA | 18 | 56 |

## 2.4 Conclusions

- Critical micellar concentration (CMC), degree of binding of counterions to the micelles (β) and surface properties such as surface excess concentration ($\Gamma_{max}$) and minimum area per molecule ($A_{min}$) at the air/water interface of bis-cationic surfactants strongly depend on head group polarity.
- The increase in head group polarity of butane1,4-bis(dodecyldimethyl ammonium bromide) surfactant by increasing the number of $-C_2H_4OH$ groups per molecule in place of $-CH_3$ groups at quaternary ammonium head of surfactant molecule results in drastic decrease in CMC values from $1.3 \times 10^{-3}$ to $2.7 \times 10^{-5}$ to $7.9 \times 10^{-6}$ M and increase in binding (β) of counterion from 0.68 to 0.74 to 0.80.
- The sharp decrease in effective Gibbs free energy change ($\Delta G^{\circ}_{eff}$) indicates that the increase in head group polarity of bis-cationic surfactants enhances the micellization process than adsorption.
- The thermodynamic parameters of micellization indicate that the micellization process is entropy driven.
- The increase in intrinsic viscosity (η), hydration of micelles ($h_m$) and shape factor (ν) with increase in head group polarity, indicate growth of micelle.
- SANS studies show that the aggregation number (N) and dimension of micelles (b/a) increase with increase in head group polarity and concentration of surfactant.

## 2.5 Literature Cited


1. Fisicaro E., Pelizzetti E., Viscardi G., Quagliotto P., Trossarelli L., *Colloids Surfaces A*, **1994** *84,*59.
2. Rosen M. J., Mathias J. H., Davenport L.,*Langmuir*, **1999,***15,* 7340
3. Song Li D., Rosen M. J., *Langmuir,* **1996,** *12,* 1149.
4. De S., Aswal V. K., Goyal P. S., Bhattacharya S., *J. Phys. Chem.,* **1996,***100,* 6152.
5. Aswal V. K., Halder J., Goyal P. S., Bhattacharya S., *Appl. Phys. A,* **2002,***74,* 354.
6. Menger F. M., Keiper J. S., Mbadugha B. N. A., Caran K. L., Romsted L. S., *Langmuir,* **2000,***16,* 9095.
7. Renouf P., Mioskowski C., Lebeau L., Hebrault D., Desmurs J. R., *Tetrahedron Lett.,* **1998,** *39,* 1357.
8. Oda R., Hue I., Candau S. J., *Chem. Comm.,* **1997**, *21*,2105.
9. Rosen M. J., Gao T., Nakatsuji Y., Masuyama A., *Colloids Surfaces A*, **1994,** *88*, 1.
10. Zana R. Levy H., Papoutsi D., Beinert G., *Langmuir,* **1995**, *11*, 3694.
11. Menger F. M., Peresypkin A. V., *J. Am. Chem. Soc.,* **2001**,*183*, 539.
12. Rosen M. J., *Chmtech,* **1993,** *23* , 30.
13. Rosen M. J., *Surfactants and Interfacial Phenomenon*, 2nd Ed., John Wiley, New York, **1988.**
14. Bunton C.A., Robinson L., Schaak J., Stern M. F., *J. Org. Chem.,* **1971**,*36,* 2346.
15. Srivastava S. K., Singh Th. R., *J. Surface Sci. Technol.* **1998**,*14* , 48.
16. El Achouri M., Kertit S., Gouttaya H. M., Nciri B., Bensouda Y., Perez L., Infante M.R., Elkacemi K., *Prog. Org. Coatings,* **2001**, *43,* 267.
17. Sharma V., Borse M., Jauhari S., Pai K. B., Devi S., *Tenside Surf. Det.,* **2005**, *42,* 3.
18. Kopecky F., *Pharmazie,* **1996**, *51,* 135.

19. Dinino F., Muthard D. A., Sazmann T. N., *Bioorg. Med. Chem. Lett.*, **1993**, *3,* 2187.
20. Karlsson L., Marcel C. P., Van E., Olle S., *J. Colloid Interface Sci.*, **2003**, *252,* 290.
21. Kremer A. C., Edwards A. J., Jennings K. H., Jenkins O., Marshall I., McGregor C., Neville W., Rice S. Q., Smith R. J., Wilkinson M. J., Kirby A., *Chem. Commun.*, **2002**,*14*,1253.
22. Dubnickova M., Bobrowaka M., Soederstroem T., Iglic A., Haegerstrand H., *Acta Biochemica Polonica,* **2000**, *47,* 651.
23. Collart O., Van der Voort P., Vansant E. F., Desplantier D., Galarneau A., Di Renzo F., Fajula F., *J. Phys. Chem. B,* **2001**, *105,* 12771.
24. Huo Q., Margolese D.I., Stucky G. D., *Chem. Mater,* **1996**, *8,* 1147.
25. Van Der Voort P., Mathieu M., Mees F., Vansant E. F., *J. Phys. Chem. B.,* **1998**, *102,* 8847.
26. Rosen M. J., *J. Am. Oil Chem. Soc.,* **1972**, *49* , 293.
27. Sulthana S. B., Bhat S. G. T., Rakshit A. K., *Langmuir,* **1997**,*13,* 4562.
28. Thomas H. G., Lomakin A., Blankschtein D., Benedek G. B., *Langmuir,* **1997**, *13,* 209.
29. Schott H., *J. Colloid Interface Sci.,* **1995**, *173,* 265.
30. Vojtekova M., Kopecky F., Greksakova O., *Collect. Czech. Chem. Commun,* **1994**, *59,* 99.
31. Mukerjiee P., Mysels K. J., *"Critical Micellar Concentrations of Aqueous Surfactant Systems"*, National Bureau of Standards; Washington, DC, USA, **1971**.
32. Sulthana S. B., Rao P. V. C., Bhat S. G. T., Rakshit A. K., *J. Phys. Chem. B,* **1998**,*102* , 9653.
33. Hirata H., Hattori N., Ishida M., Okabayashi H., Frusaka M., Zana R., *J. Phys. Chem. B,* **1995**, *99,* 17778.
34. Zana R., *Adv In Colloid and Interface Sci.,* **2002**, *97,* 203.
35. Dreja M., Pyckhout-Hintzen W., Mays H., Tieke B., *Langmuir,* **1999**, *15,* 391.
36. M. J. Rosen, *J. Am. Oil Chem. Soc.,* **1972**, *19,*293.

37. Li D. Song and Milton J. Rosen, *Langmuir,* **1996**, *12,* 1149
38. R. Zana, Y.Talmon, *Nature,* **1993,** *362,* 288.
39. R. Zana, *Langmuir,* **1996,***12*, 1208
40. Wettig S. D., Li X., Verrall R. E., *Langmuir,* **2003**,*19,* 3666.
41. Wettig S. D., Nowak P., Verrall R.E., *Langmuir,* **2002**,*18,* 5354.
42. Wettig S. D., Verrall R. E., *J. Colloid Interface Sci.,* **2001**, *235* ,310.
43. Zana R., *Langmuir,* **1996**,*12,* 1208.
44. Menger F. M., Keiper J. S., *Angew. Chem., Int. Ed.,* **2000**, *39,* 1907.
45. Halder J., Aswal V. K., Goyal P. S., Bhattacharya S., *Angew Chem., Int. Ed.* **2001,** *40*,1228.
46. Shah D. O., *J. Colloid Interface Sci,* **1971**, *37*, 744
47. Chen S. H., *Annu., Rev. Phys. Chem.* **1986**, *37* , 351
48. Aswal V. K., Goyal P. S., *Current Science,* **2000**, *79*, 947.
49. Pedersen J. S., *Adv. Colloid Interface Sci.,* **1997,** *70*,171.
50. Zana R., *J. Colloid Interface Sci.,* **2002**, *252,* 259.
51. Rosen M. J., Song Li D., *J. Colloid Interface Sci.,* **1996**,*179,* 261.
52. Patist A., Bhagwat S.S., Penfield K. W., Aikens P., Shah D.O., *J. Surf. Deteergent*, **2000**, *3,* 53.
53. Shinod K., Nakagawa T., *Colloidal Surfactants; Some physicochemical properties*, Academic press, New York, **1963**.
54. Hunter R.I., *Foundations of Colloid Science,* Oxford University press, Oxford, *Vol.1,* **1987**.
55. Van Os N. M., Smitt B., Karaboni S. K., *Recl. Tran. Chim. Pays-Bas,* **1994,***113*, 181.
56. Camesano T. A., Nagarajan R., *Colloids and Surfaces A.,* **2000**,*167,* 165.
57. Nusselder J. J. H., Engberts J. B. F. N., *J. Colloid Interface Sci.,* **1992**, *148,* 353.
58. Chattoraj D. K., Birdi K. S., *Adsorption and the Gibbs Surface Excess,* Plenum Press New York, 22, **1984**.

59. Anand K., Yadav O. P., Singh P. P., *Colloids and Surfaces A.*, **1991**, *55*, 345.

60. Rosen M. J., Cohen A.W., Dahanayabi M., Hua X., *J. Phys. Chem.*, **1982**, *86*, 541.

61. Rybicki E., *Tenside. Surf. Det.*, **1990**, *27*, 336.

62. Mukerjee P., *J. Colloid Sci.*, **1964**,*19*, 722.

63. Tokiwa F., Ohki K., *J. Phys. Chem.*, **1967**, *71*, 1343.

64. Oncley J. L., Ann. N. Y. *Acad. Sci.*, **1949**, *41*, 121.

65. Simha R., *J. Phys. Chem.*, **1940**, *44*, 25.

66. Hayter J. B., Penfold J., *Colloid Polym. Sci,.* **1983**, *261*, 1022.